PCCP

Accepted Manuscript

ROYAL SOCIETY OF CHEMISTRY

www.rsc.org/pccp

Physical Chemistry Chemical Physics
CREATED USING THE RSC LaTeX PCCP ARTICLE TEMPLATE – SEE www.rsc.org/electronicfiles FOR DETAILS
ARTICLE TYPE www. rsc.org/xxxxxx | XXXXXXXX

Conducting behavior of chalcopyrite-type $CuGaS_2$ crystals under visible light

Jorge L. Cholula-Díaz,[a] José Barzola-Quiquia,*[b] Christian Kranert,[b] Tom Michalsky,[b] Pablo Esquinazi,[b] Marius Grundmann[b] and Harald Krautscheid[a]

Received Xth XXXXXXXXXX 20XX, Accepted Xth XXXXXXXXX 20XX
First published on the web Xth XXXXXXXXXX 200X
DOI: 10.1039/b000000x

Millimeter size high quality crystals of $CuGaS_2$ were grown by chemical vapor transport. The highly ordered chalcopyrite structure is confirmed by X-ray diffraction and Raman spectroscopy. According to energy dispersive X-ray spectroscopy the composition of the crystals is very close to the formula $CuGaS_2$. Room temperature photoluminescence measurements indicate the presence of an emission peak at about 2.36 eV that can be related to a donor-acceptor pair transition. The electrical resistance as a function of the temperature is very well described by the Mott variable range hopping mechanism. Room temperature complex impedance spectroscopy measurements were performed in the alternating current frequency range from 40 to 10^7 Hz in dark and under normal light. According to the impedance spectroscopy data the experimental results can be well described by two circuits in series, corresponding to bulk and grain boundary contributions. An unusual positive photoresistance effect is observed in the frequency range between 3 and 30 kHz, which we suggest to be due to intrinsic defects present in the $CuGaS_2$ crystal.

1 Introduction

The ternary chalcopyrite compounds with the general formula $CuME_2$ (M = In, Ga; E = S, Se) are semiconductors with direct band gaps in the range suitable for photovoltaic applications. Solar cells based on Cu(In,Ga)Se_2 thin-films have demonstrated to yield efficiencies beyond 20% in the laboratory,[1] which makes this type of materials very attractive to be used in large-area solar modules.[2] Since the first report of the synthesis and structural characterization of ternary chalcopyrites,[3] extensive studies have been carried out to investigate their physical and chemical properties. Among this family of materials, $CuGaS_2$ has a direct band gap of about 2.40 eV at room temperature,[4] very close to the optimum band gap of 2.41 eV for the realization of intermediate band solar cells with a theoretical limiting efficiency of 46% under 1 sun illumination.[5] Furthermore, $CuGaS_2$ has also been considered a good candidate for applications in visible light-emitting devices. For this reason, heterodiodes involving p-type (p) $CuGaS_2$ with n-type (n) CdS,[6] Al[7] and more recently, n-GaP[8] were made. Resistivity, Hall coefficient and Hall mobility in the temperature range $77-400$ K revealed that intrinsic defects are the important factors controlling the electrical properties of p-$CuGaS_2$ single crystals.[9] The photoconductivity (PC) spectra of undoped p-$CuGaS_2$ crystals, with dark resistivity of $\sim 10^3$ Ω·cm at room temperature, exhibit sharp peaks in the band edge range related to a band-to-band transition and a band-to-shallow donor transition.[10] The observed polarization dependence of the PC spectra is indicative of crystal field splitting.[11]

Previously, positive photoresistance effect was observed in several semiconductor materials/systems such as Co-doped Si,[12] GaAs/AlGaAs,[13] p-type $Cd_xFe_{1-x}Se$,[14] Ga-doped PbTe,[15] amorphous Se,[16] γ-In_2S_3[17] and ZnO.[18] In most cases, the explanation for this effect has been the reduction of the major carrier concentration due to impurities levels, which act as recombination centers. To our knowledge the positive photoresistance effect has not been reported for $CuGaS_2$.

Alternating current (a.c.) impedance spectroscopy (IS) has been considered as a powerful alternative method to characterize the electrical properties of materials.[19] IS measurements are done over a wide range of frequencies, typically from 10^{-2} to 10^7 Hz, and the different regions of the sample are identified according to their electrical relaxation times or time constants.[20] In the solar cell technology, this technique has been used to find equivalent circuits, which describe the structure and operation of the device under illumination, as in the case of CdTe/CdS photovoltaic structures.[21]

The aim of this work was to investigate the electrical transport properties of chalcopyrite-type $CuGaS_2$ crystals as a function of the temperature and the complex impedance be-

[a] *Institut für Anorganische Chemie, Universität Leipzig, Johannisallee 29, 04103 Leipzig, Germany.*
[b] *Institut für Experimentelle Physik II, Universität Leipzig, Linnéstr. 5, 04103 Leipzig, Germany. Fax: +49 (0)341 9732769; Tel: +49 (0)341 9732765; E-mail: j.barzola@physik.uni-leipzig.de*

havior in dark and under white light illumination of the sample at room temperature. The changes of the resistance at specific a.c. frequencies allowed us the determination of the frequency range in which the negative and positve photoresistance effects can be observed, as well as the mechanisms dominating the transport properties in our crystals.

2 Experimental section

$CuGaS_2$ crystals were synthesized by the iodine vapor transport method[22]. A mixture of Cu_2S (201 mg, 1.3 mmol) and Ga_2S_3 (297 mg, 1.3 mmol) was sealed in a quartz ampoule (length 10 cm and diameter 1.5 cm) along with I_2 (8.4 mg·cm^{-3}). The ampoule was placed in a two zone horizontal oven with a source temperature (T_S) of 940 °C and a growth temperature (T_G) of 800 °C verified by a thermocouple type K. The crystals were allowed to grow for three days and the product was washed with acetone and diluted HCl. Crystals with a dark green color and average size of 600 x 600 x 300 μm^3 were obtained. A typical as-grown $CuGaS_2$ crystal is shown in Fig. 1.

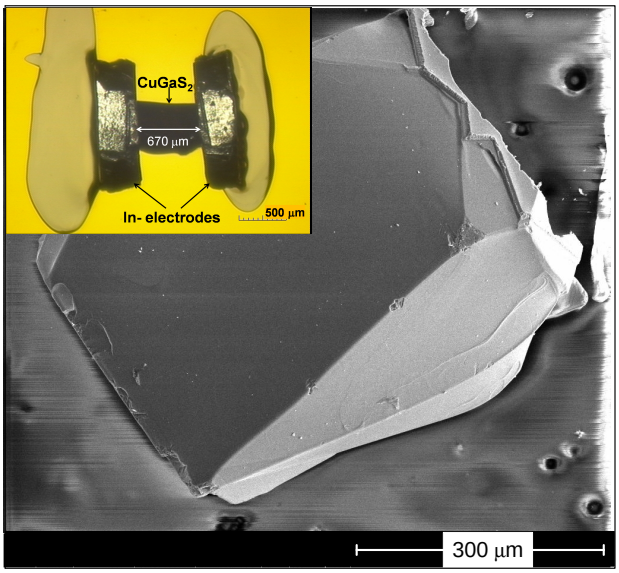

Fig. 1 Top-view SEM image of an as-grown $CuGaS_2$ crystal. Inset: Position of the In-electrodes on the $CuGaS_2$ crystal.

X-ray powder diffraction (XRD) patterns were measured on a STOE Stadi P diffractometer in Debye-Scherrer mode with Cu $K_{\alpha 1}$ radiation ($\lambda = 1.540598$ Å) at room temperature. The data were recorded with a linear PSD over the 2θ range of 5 to 90°.

Raman spectroscopy of a $CuGaS_2$ crystal was carried out at room temperature under ambient conditions in backscattering geometry. The sample was excited by the light of a frequency-doubled solid state laser emitting at $\lambda = 532$ nm. The laser light was focused by means of a 50x microscope objective with a numerical aperture of NA= 0.42 onto the sample and the scattered light was collected by the same objective. We used a Jobin Yvon U1000 double spectrometer (focal length of 1m) equipped with two 2400 l·mm^{-1} gratings and a liquid nitrogen cooled CCD with a pixel pitch of 13.5 μm for spectral dispersion and detection. The slit width used for these measurements corresponds to a spectral resolution of 0.4 cm^{-1}. For polarization dependent measurements, we used an achromatic $\lambda/2$ waveplate positioned between beamsplitter and objective. Thereby, the polarization of the incident light was rotated with respect to the sample and the collected light was rotated in the opposite direction by the same angle. Because the analyzer was set fixed to be parallel to the original laser polarization, all these measurements were carried out in parallel polarized configuration.

Photoluminescence (PL) measurements were carried out using continuous wave HeCd laser radiation at 325 nm for nonresonant excitation. The PL signal was collected by using a numerical aperture NA= 0.4 UV-Vis objective. For spectral resolution the signal was transferred to a spectrometer with a 320 mm focal length.

Scanning electron microscopy (SEM) images and elemental analysis by means of energy dispersive X-ray (EDX) were measured using a FEI nanolab200 microscope. For measuring the transport properties, a crystal with size of 670 x 500 x 100 μm^3 was contacted with Indium electrodes (see inset Fig. 1) and mounted on the cold head of a standard closed cycle refrigerator inside a vacuum bell, with a minimum temperature of 25 K.

The impedance spectroscopy (IS) measurements were carried out at room temperature in the darkness and under normal white light produced by an incandescent light bulb (typical luminance $\sim$ 500 lx and power density $\sim$ 1 W·cm^{-2}). The measurements of the IS were done using an Agilent 4294-A Impedance Analyzer over the frequency (f) range of 40 Hz to 10 MHz and at constant frequencies exploring the time dependence in the response. Each measurement was done using alternating current (a.c.) signals with an excitation voltage of 1 V.

3 Results and discussion

3.1 Structural and optical properties

The XRD pattern of milled $CuGaS_2$ crystals in Fig. 2 shows a single phase tetragonal chalcopyrite (CH) structure (space group $I\bar{4}2d$)[3] with lattice parameters $a = 5.35$ Å and $c = 10.49$ Å, which are in agreement with those values reported for stoichiometric $CuGaS_2$ ($a = 5.35$ Å and $c = 10.47$ Å).[23] However, twinning of the crystals prevented us from determining

the crystallographic orientations of its faces.

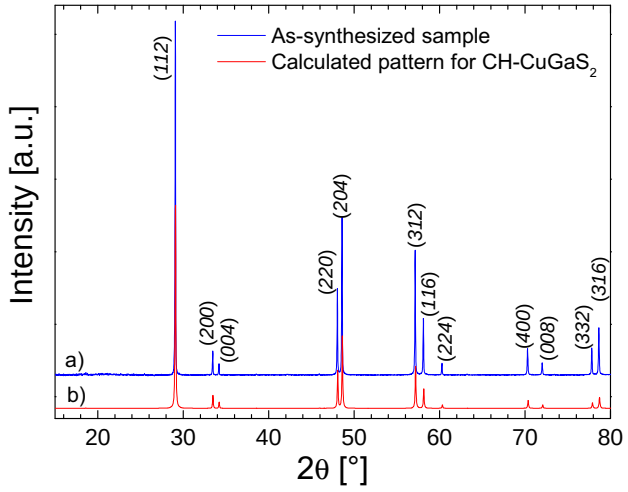

Fig. 2 XRD diffraction pattern (linear intensity scale) of a) milled $CuGaS_2$ crystals and b) calculated pattern for chalcopyrite type (CH) $CuGaS_2$ based on single crystal data.[23]

EDX measurements of the as-grown crystals (spectrum shown in Fig. 3) give an atomic composition of 25.7% Cu, 25.5% Ga and 48.8% S, which is in agreement with the formula $CuGaS_2$.

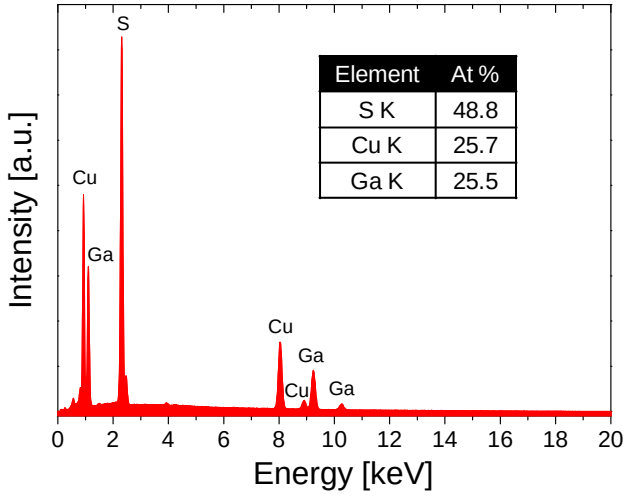

Fig. 3 EDX analysis of an as-grown $CuGaS_2$ crystal.

The room temperature PL spectrum of as-grown $CuGaS_2$ crystals is shown in Fig. 4. The main PL signal is observed at about 2.36 eV. This emission peak may correspond to a recombination of an acceptor-donor pair.[24–26] In $CuGaS_2$, Cu and S vacancies act as an intrinsic acceptor and as a compensating donor, respectively.[9,27] The crystals may have a large number of these two vacancies raising the density of acceptor-donor pairs, which make the observation of this emission peak possible. The strong broadening of the PL peak is due to the strong increase of the exciton (electron)-phonon interaction at room temperature.[28] Similar experimental tendencies have been observed in temperature dependence of photoluminescence measurements of $CuGaS_2$ crystals[29,30] and $CuGaS_2$ films epitaxially grown on Si(111) substrates.[28]

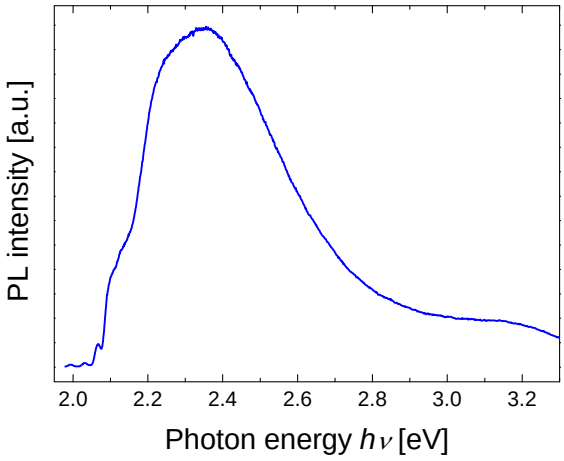

Fig. 4 Photoluminescence (linear intensity scale) recorded at room temperature of an as-grown $CuGaS_2$ crystal.

The Raman spectrum is dominated by a very strong line at 311 cm^{-1} exhibiting A_1 symmetry (see Fig. 5). This is in very good agreement to Raman spectra reported in the literature.[31–33] Also the other modes observed by us agree well with those found previously. The observed polarization dependence of the individual phonon modes results from their respective symmetry. Due to twinning of the crystal we could not unambiguously determine the symmetries of the other phonon modes observed by us from their polarization dependent behavior. However, the dependence of the peak intensities on the polarization direction showed only a two-fold symmetry (see inset of Fig. 5) which substantiates the high crystalline quality of the sample.

3.2 DC electrical properties

The electrical behavior of the sample-electrode system was checked by measuring its characteristic current-voltage ($I-U$) curves at 300 K. The contacts showed a linear, Ohmic response in a wide range of voltage, see Fig. 6b. Thus, the In-electrodes ensured the possibility to carry out reproducible impedance spectroscopy measurements.

Temperature dependent measurements of the resistance $R(T)$ were performed in the temperature range of $200-300$ K, see Fig. 6. At lower temperatures the resistance increased to values over the range of our devices. The temperature de-

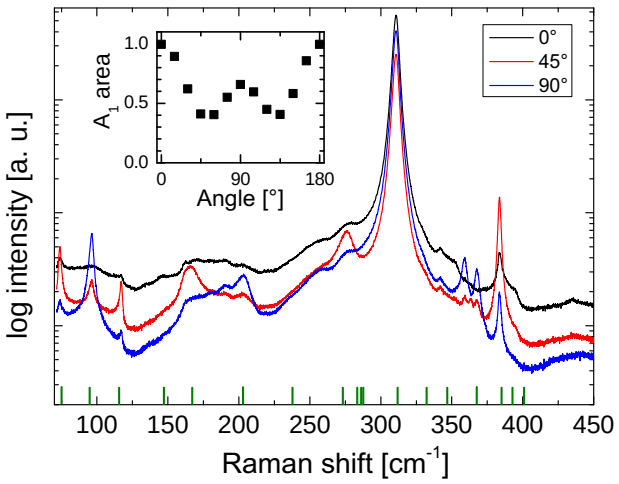

Fig. 5 Raman spectrum of a $CuGaS_2$ crystal in parallel polarized backscattering geometry. The green bars at the bottom mark the phonon energies reported by Carlone *et al.*[32] The inset shows the normalized area of the A_1 peak in dependence on the polarization angle which is given relative to the direction the highest A_1 intensity was observed for.

pendence of the resistance $R(T)$ in the measured temperature range follows the variable range hopping (VRH) mechanism described by the equation:

$$R(T) = R_0 \cdot exp\left[(T_0/T)^{1/p}\right] \quad (1)$$

where R_0 is a prefactor and T_0 is a characteristic temperature coefficient. The value of p depends on the nature of the hopping process, e.g., in the case in which the density of states $N(E_F)$ at the Fermi level E_F is constant, the VRH resistance is expressed with $p = 4$ according to Mott.[34] Taking into account Mott′s law, the characteristic temperature coefficient T_0 depends on the density of states $N(E_F)$ at the Fermi level in the form[35]

$$T_{0,Mott} = \frac{18}{k_B \xi^3 N(E_F)} \quad (2)$$

where ξ is the localization length and k_B is the Boltzmann constant. The experimental data of the temperature dependence of the resistance $R(T)$ can be well fitted using Eq. 1, see Fig. 6. From the fitting curve a value for the characteristic temperature coefficient of $T_0 = 1.81 \cdot 10^9$ K was obtained, and assuming a typical value for the density of states $N(E_F) \approx 10^{19}$ $eV^{-1} \cdot cm^{-3}$ for chalcopyrite semiconductor materials,[36] a localization length $\xi \approx 0.2$ nm was obtained, which is agreement with typical values found in the literature (0.3 – 3 nm).[37]

3.3 Dynamic properties

Impedance spectroscopy measurements on a $CuGaS_2$ crystal were carried out at room temperature under an incandescent

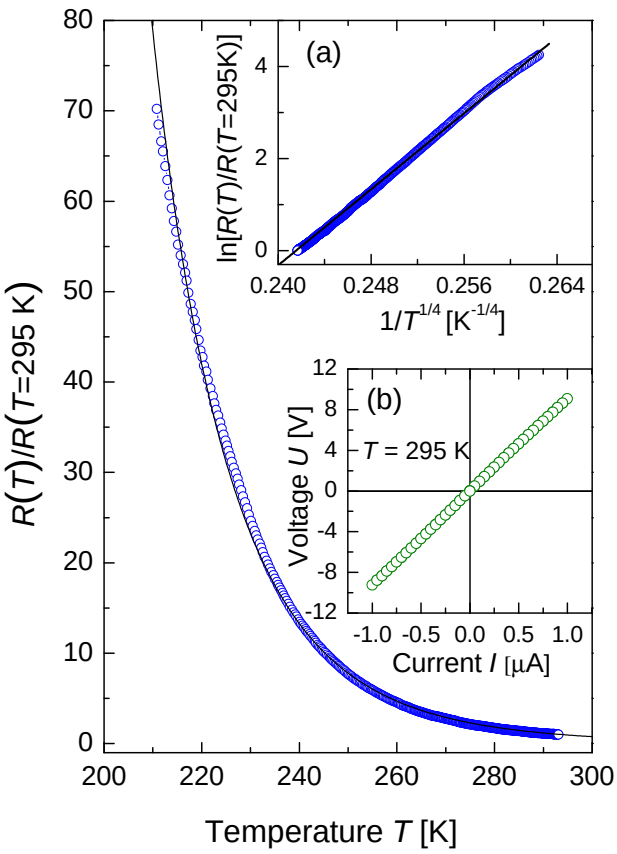

Fig. 6 Temperature dependence of the resistance $R(T)$ of a $CuGaS_2$ crystal. Insets: a) ln[$R(T)$] versus $T^{-1/4}$ and b) characteristic $I-U$ curve of the same sample recorded at 295 K showing ohmic behavior. Solid lines are the fitting curves according to Eq. 1 to the experimental data.

light bulb and in darkness. In a first experiment, the photoresistance effect at a constant a.c. frequency of $f = 75$ Hz was investigated on a $CuGaS_2$ crystal. The rate of change of the resistance with respect to the time was measured when light with typical luminance of ~ 500 lx was repeatedly switched on and off, as shown in Fig. 7. Here is to observe a quick decrease of the resistance of $\sim 20\%$ in the first two seconds of illumination. The recovery of the initial state of the resistance is relatively quick. In the same Fig. 7 the reversibility of the photoresistance effect is demonstrated.

In a second experiment the a.c. frequency dependence of the resistance $R(f)$ of the sample in darkness and under illumination at different periods of time was investigated, the results of the impedance Z' and reactance Z'' are shown in Fig. 8. In the low frequency range (40 Hz $< f <$ 3 kHz), significant changes in the negative photoresistance effect as function of the illumination times are observed. For the intermediate frequency range (3 kHz $< f <$ 30 kHz) an unexpected posi-

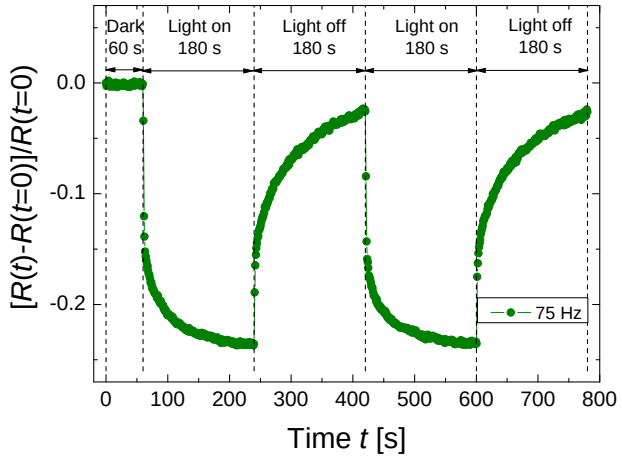

Fig. 7 Photoresistance measurements performed on a $CuGaS_2$ crystal using a fixed a.c. frequency of $f = 75$ Hz.

tive photoresistance is observed. These experimental results are discussed in more detail together with the photoresistance effect measurements at different fixed frequencies. For $f > 30$ KHz no difference between darkness and illumination are seen within the experimental accuracy.

The experimental impedance results can be well described using a simple equivalent circuit consisting of two circuit units connected in series; each of them is described by a capacitor and a resistor in a parallel circuit. The resistance Z' can be expressed as follows

$$Z' = \frac{R_1}{1+R_1^2 f^2 C_1^2} + \frac{R_2}{1+R_2^2 f^2 C_2^2} \quad (3)$$

and the expression for the reactance Z is

$$Z'' = \frac{R_1^2 f C_1}{1+R_1^2 f^2 C_1^2} + \frac{R_2^2 f C_2}{1+R_2^2 f^2 C_2^2} \quad (4)$$

where R_1, R_2 and C_1, C_2 are the resistance and capacitance for circuit 1 and 2, respectively (see inset of Fig. 8a).

In Fig. 9 the experimental Cole-Cole plots (Z' vs Z'') are shown together with their respective fitting curves (solid lines) and the values obtained for the best-fitting parameters of the equivalent circuit describing the experimental results are listed in Table 1.

According to their capacitance values, the circuit 1 (R_1-C_1) can be related to the contribution of the grain boundaries and the circuit 2 (R_2-C_2) to the bulk properties of the crystal.[20] It is noticed that the contribution due to grain boundaries is more sensitive to the illumination than the bulk contribution. According to the photoluminescence results, our $CuGaS_2$ crystal has a relative high density of vacancy defects, which in general are predominantly present at the grain boundaries.[38,39]

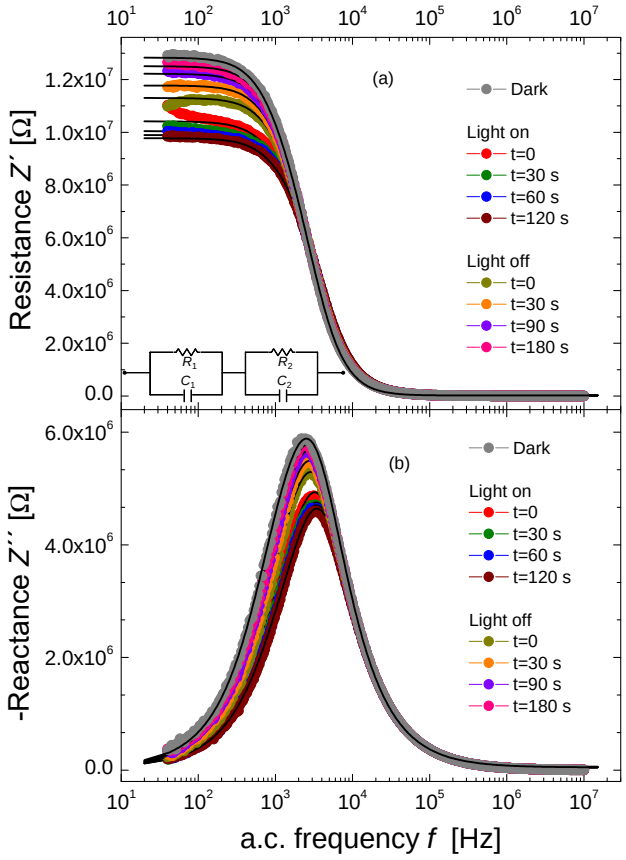

Fig. 8 IS measurements on a $CuGaS_2$ crystal: a) resistance Z' and b) reactance Z'' as a function of a.c. frequency f. Solid lines are the fitting curves according to Eqs. 3 and 4 to the experimental data in a) and b), respectively. Inset in a) is the equivalent circuit modeled for the IS experimental data.

Assuming that the density of defects levels are shallow and non-discrete, the applied white light excites more effectively the electronic transitions between acceptor or donor levels and the bands than the fundamental electronic transition between states at the band edges.

In a final experiment, the transient photoresistance effect at different fixed frequencies was investigated in order to get information about the relaxation times (τ) involved in the process. In Fig. 10 the experimental results together with the fitting curves are plotted. The rate of change of the resistance with respect to the time (t), either under illumination (light on, L_{on}) and after illumination (light off, L_{off}) can be expressed as the sum of two exponential functions:

$$\frac{R(t)-R(t=0)}{R(t=0)} = A + a \cdot exp\left(-\frac{t-b}{\tau_1}\right) + c \cdot exp\left(-\frac{t-d}{\tau_2}\right) \quad (5)$$

where a and c are pre-exponential factors and, A, b and d

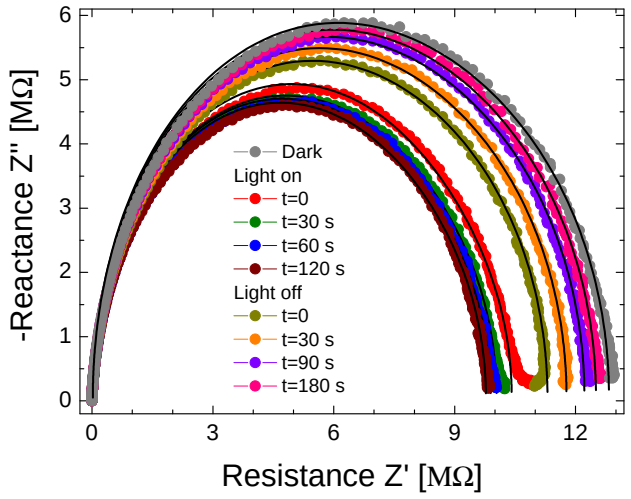

Fig. 9 Cole-Cole plots of IS measurements on a $CuGaS_2$ crystal in darkness, under illumination (light on) and in darkness after illumination (light off). Solid lines are the fitting curves according to Eq. 3 and 4 to the experimental data.

Table 1 Best-fitting parameters describing the equivalent circuit proposed for the impedance spectroscopy results presented in Fig. 9

Condition	R_1 [MΩ]	C_1 [F]	R_2 [MΩ]	C_2 [F]
Darkness	3.4	$2.7{\cdot}10^{-10}$	9.4	$3.5{\cdot}10^{-11}$
Light on				
$t = 0$	1.3	$8.1{\cdot}10^{-10}$	9.1	$3.2{\cdot}10^{-11}$
$t = 30$ s	1.4	$6.6{\cdot}10^{-10}$	8.6	$3.2{\cdot}10^{-11}$
$t = 60$ s	1.2	$8.0{\cdot}10^{-10}$	8.7	$3.2{\cdot}10^{-11}$
$t = 120$ s	1.3	$6.6{\cdot}10^{-10}$	8.4	$3.2{\cdot}10^{-11}$
Light off				
$t = 0$	3.0	$2.4{\cdot}10^{-10}$	8.3	$3.5{\cdot}10^{-11}$
$t = 30$ s	2.9	$2.8{\cdot}10^{-10}$	8.8	$3.5{\cdot}10^{-11}$
$t = 90$ s	3.2	$2.7{\cdot}10^{-10}$	9.0	$3.5{\cdot}10^{-11}$
$t = 180$ s	3.2	$2.8{\cdot}10^{-10}$	9.3	$3.5{\cdot}10^{-11}$

are free parameters. τ_1 is related to the relative sharp decreasing of the resistance when the lamp is switched on (L_{on}). The decrease in the resistance occurs in an interval of time $\tau_1 = 1.2 \pm 0.2$ s for all the a.c. frequencies. The term τ_2 gives the relaxation times, which are in the range of $\tau_2 = 37 \pm 1$ s. For the changes in the resistance observed after illumination (L_{off}), Eq. 5 also describes well the experimental data. In this case, τ_1 is substituted by τ_3 and τ_2 by τ_4. Both characteristic times τ_1 and τ_3 have similar values and are related to the rate of generation and recombination of charge carriers, respectively.[40,41] The term τ_4 has values in the range of 60 ± 5 s and is related to the carrier lifetime taking into account that this characteristic time corresponds to the mechanism of the slow exponential increase of the photoresistance.[40,42]

The increase of the resistance upon illumination of the $CuGaS_2$ crystal was observed in the a.c. frequency range 3 kHz $< f <$ 30 kHz. This response can be explained by the reduction of the majority carrier due to a recombination process.[43] For this model to be valid in a p-type semiconductor material, it is mandatory that a shallow level is localized near the conduction band and a deep level lies under the Fermi level in the energy band structure. Minority carriers (electrons in the case of p-type $CuGaS_2$) formed from the deep level upon illumination recombine with majority carriers in the shallow level, which acts as a recombination center. We assume that the capture cross section for electrons (and holes) of this ionized donor like trap is substantially enhanced or activated due to a resonance process between a hole plasma (present in the donor like trap as also observed in the semiconductor GaAs[13]) and the frequency of the a.c. signal. This overall process reduces the free carrier density in the presence of light and in a certain a.c. frequency range. Further experiments need to be carried out in order to corroborate these assumptions.

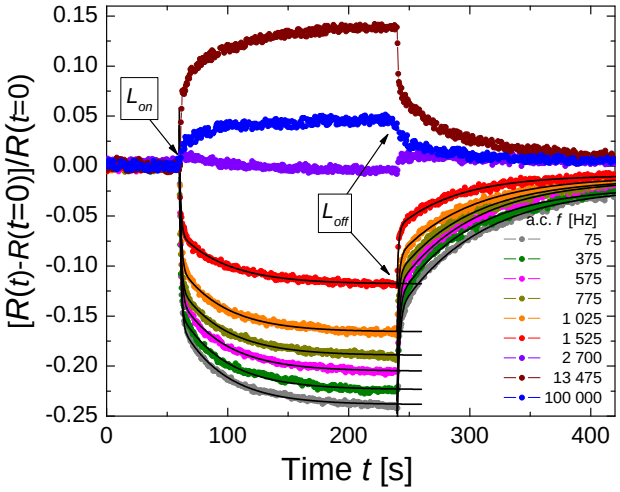

Fig. 10 Photoresistance effect as a function of the a.c. frequency f. L_{on} and L_{off} indicate the switch on and off of the lamp at time $t = 60$ s and $t = 240$ s, respectively. Solid lines are the fitting curves according to Eq. 5 to the experimental data.

4 Conclusions

We have investigated the electrical transport properties of $CuGaS_2$ crystals using impedance spectroscopy. XRD patterns and Raman spectroscopy together with elemental analysis by means of EDX show that our crystals are composed of single-phase chalcopyrite $CuGaS_2$. The relative changes of the resistance of the sample under illumination are in the order of 25%. This photoresistance effect is relative quick, which makes the semiconductor $CuGaS_2$ attractive for future applications as photodetector in the visible range. The impedance

spectroscopy shows different responses according to the frequency of the alternating current signal, i.e. when the $CuGaS_2$ crystal is illuminated with white light and frequencies less than 3 kHz the resistance decrease, but using frequencies in the range of $3 - 30$ kHz an unusual increase in the resistance is observed. These results are interpreted assuming the presence of a high density of defect levels in the sample.

Acknowledgement

J.L. Cholula-Díaz thanks Graduate School of Natural Sciences "BuildMoNa" of Universität Leipzig for a fellowship. Financial support by Universität Leipzig and PbF-1 is gratefully acknowledged. C. Kranert was funded by the European Union and the Free State of Saxony.

References

1 P. Jackson, D. Hariskos, E. Lotter, S. Paetel, R. Wuerz, R. Menner, W. Wischmann and M. Powalla, *Prog. Photovolt: Res. Appl.*, 2011, **19**, 894–897.
2 M. Powalla, M. Cemernjak, J. Eberhardt, F. Kessler, R. Kniese, H. D. Mohring and B. Dimmler, *Sol. Energy Mater. Sol. Cells*, 2006, **90**, 3158–3164.
3 H. Hahn, G. Frank, W. Klingler, A. D. Meyer and G. Störger, *Z. Anorg. Allg. Chem.*, 1953, **271**, 153–170.
4 B. Tell and J. L. Shay, *Phys. Rev. B*, 1971, **4**, 2463–2471.
5 A. Martí, D. Fuertes Marrón and A. Luque, *J. Appl. Phys.*, 2008, **103**, 073706.
6 S. Wagner, *J. Appl. Phys.*, 1974, **45**, 246–251.
7 S. Kobayashi, Y. Momiyama and F. Kaneko, *Jpn. J. Appl. Phys.*, 1992, **31**, L1606–L1608.
8 T. Honda, K. Hara, J. Yoshino and H. Kukimoto, *J. Phys. Chem. Solids*, 2003, **64**, 2001–2003.
9 P. W. Yu, D. L. Downing and Y. S. Park, *J. Appl. Phys.*, 1974, **45**, 5283–5288.
10 M. Susaki, H. Horinaka and N. Yamamoto, *Jpn. J. Appl. Phys.*, 1991, **30**, 2797–2801.
11 B. Tell and H. M. Kasper, *Phys. Rev. B*, 1973, **7**, 740–742.
12 C. M. Penchina, J. S. Moore and N. Holonyak Jr., *Phys. Rev.*, 1996, **143**, 634–636.
13 M. J. Chou, D. C. Tsui and G. Weimann, *Appl. Phys. Lett.*, 1985, **47**, 609–611.
14 N. V. Joshi, L. Mogollon, J. Sanchez and J. M. Martin, *Solid State Commun.*, 1988, **65**, 151–153.
15 B. A. Akimov, V. A. Bogoyavlenskiy, L. I. Ryabova and V. N. Vasil´kov, *Phys. Rev.*, 2000, **61**, 16045–16051.
16 Br. Petrėtis and M. Balčiūnienė, *J. Non-Cryst. Solids*, 2002, **311**, 42–47.
17 R. Sreekumar, R. Jayakrishnan, C. S. Kartha and K. Vijayakumar, *J. Appl. Phys.*, 2006, **100**, 033707.
18 H. Kim, S. Kim, C. Kim and S.-H. Choi, *Thin Solid Films*, 2009, **518**, 305–308.
19 E. Barsoukov and J. R. Macdonald, *Impedance Sprectroscopy: Theory, Experiment, and Applications*, John Wiley & Sons, Inc., New Jersey, 2005.
20 J. T. S. Irvine, D. C. Sinclair and A. R. West, *Adv. Mater.*, 1990, **2**, 132–138.
21 Y. Y. Proskuryakov, K. Durose, M. K. Al Turkestani, I. Mora-Seró, G. Garcia-Belmonte, F. Fabregat-Santiago, J. Bisquert, V. Barrioz, D. Lamb, S. J. C. Irvine and E. W. Jones, *J. Appl. Phys.*, 2009, **106**, 044507.
22 N. Yamamoto, N. Tohge and T. Miyauchi, *Jpn. J. Appl. Phys.*, 1975, **14**, 192–196.
23 S. C. Abrahams and J. L. Bernstein, *J. Chem. Phys.*, 1973, **59**, 5415–5422.
24 P. Rochon, E. Fortin, J. P. Zielinger and C. Schwab, *J. Phys.*, 1975, **36**, C3 67–71.
25 G. Massé, *J. Appl. Phys.*, 1985, **58**, 930–935.
26 I.-H. Choi and P. Y. Yu, *J. Phys. Chem. Solids*, 1996, **57**, 1695–1704.
27 B. Tell and H. M. Kasper, *J. Appl. Phys.*, 1973, **44**, 4988–4990.
28 J. Eberhardt, H. Metzner, Th. Hahn, U. Reislöhner, J. Cieslak, U. Grossner, R. Goldhahn, F. Hudert, G. Gobsch and W. Witthuhn, *J. Phys. Chem. Solids*, 2003, **64**, 1781–1785.
29 S. Shirakata and S. Chichibu, *J. Appl. Phys.*, 2000, **87**, 3793–3799.
30 S. Levcenco, S. Doka, V. Tezlevan, D. Fuertes Marron, L. Kulyuk, T. Schedel-Niedrig, M. Ch. Lux-Steiner and E. Arushanov, *Physica B*, 2010, **405**, 3547–3550.
31 A. Anedda, G. Bongiovanni, F. Raga, E. Fortin and M. Quintero, *Nuovo Cimento D*, 1983, **2**, 1950–1956.
32 C. Carlone, D. Olego, A. Jayaraman and M. Cardona, *Phys. Rev. B*, 1980, **22**, 3877–3885.
33 J. Gonzlez, B. J. Fernndez, J. M. Besson, M. Gauthier and A. Polian, *Phys. Rev. B*, 1992, **46**, 15092–15101.
34 N. F. Mott, *Phil. Mag.*, 1969, **19**, 835–852.
35 D. K. Paul and S. S. Mitra, *Phys. Rev. Lett.*, 1973, **31**, 1000–1003.
36 D. Abdel-Hady and A. M. Salem, *Physica A*, 1997, **242**, 141–149.
37 M. A. Majeed Khan, S. Kumar, M. Ahamed and M. S. AlSalhi, *Mater. Lett.*, 2012, **68**, 497–500.
38 J. E. Jaffe and A. Zunger, *Phys. Rev. B*, 2001, **64**, 241304.
39 S. B. Zhang and S. H. Wie, *Phys. Rev. B*, 2002, **65**, 081402.
40 R. Shukla, P. Khurana and K. K. Srivastava, *Philos. Mag. B*, 1991, **64**, 389–400.
41 N. Goyal, *Pramana-J. Phys.*, 1993, **40**, 97–105.
42 W. Fuhs and D. Meyer, *Phys. Status Solidi A*, 1974, **24**, 275–283.
43 F. Stöckmann, *Z. Phys.*, 1955, **143**, 348–356.